



Original Articles

Induction of endoplasmic reticulum stress and inhibition of colon carcinogenesis by the anti-helminthic drug rafoxanide

Federica Laudisi^{a,1}, Antonio Di Grazia^{a,1}, Veronica De Simone^b, Fabio Cherubini^a, Alfredo Colantoni^a, Angela Ortenzi^a, Eleonora Franzè^a, Vincenzo Dinallo^a, Davide Di Fusco^a, Ivan Monteleone^c, Eric R. Fearon^d, Giovanni Monteleone^a, Carmine Stolfi^{a,*}

^a Department of Systems Medicine, University of “Tor Vergata”, Rome, Italy

^b Department of Chronic Diseases, Metabolism and Ageing, Translational Research Center for Gastrointestinal Disorders, KU Leuven, Leuven, Belgium

^c Department of Biomedicine and Prevention, University of “Tor Vergata”, Rome, Italy

^d Department of Internal Medicine, Human Genetics and Pathology, University of Michigan, Ann Arbor, USA

ARTICLE INFO

Keywords:

Drug repurposing
eIF2 α
Cyclin D1
UPR
Apoptosis
Apc^{min/+} mice

ABSTRACT

Colorectal cancer (CRC) remains one of the leading causes of mortality worldwide. Drug repositioning is a promising approach for new cancer therapies, as it provides the opportunity to rapidly advance potentially promising agents into clinical trials. The FDA-approved anti-helminthic drug rafoxanide was recently reported to antagonize the oncogenic function of the BRAF V600E mutant protein, commonly found in CRCs, as well as to inhibit the proliferation of skin cancer cells. These observations prompted us to investigate the potential anti-cancer effects of rafoxanide in CRC models. We found rafoxanide inhibited proliferation in CRC cells, but not in normal colonic epithelial cells. Rafoxanide's anti-proliferative action was associated with marked reduction in cyclin D1 protein levels and accumulation of cells in the G0/G1 phase. These effects relied on selective induction of the endoplasmic reticulum stress (ERS) response in CRC cells and were followed by caspase-dependent cell death. Systemic administration of rafoxanide to Apc^{min/+} mice induced to develop CRCs caused ERS activation, proliferation inhibition and apoptosis induction in the neoplastic cells. Collectively, our data suggest rafoxanide might be repurposed as an anti-cancer drug for the treatment of CRC.

1. Introduction

Colorectal cancer (CRC) is the second leading cause of cancer-related death in the western world [1], mainly due to the lack of effective treatment in patients with advanced disease. In addition to surgery, radiotherapy and immunotherapy, chemotherapy represents a key modality for CRC treatment. Unfortunately, intrinsic and/or acquired resistance of CRC cells to chemotherapy along with the often significant side effects of commonly used cytotoxic and targeted agents represent major limitations of chemotherapy [2]. Thus, the validation of new anti-cancer agents with more pronounced efficacy against cancer and lower toxicity in normal tissues is highly desirable. As the pipeline leading to new drug development is often protracted, exacting and costly, drug repositioning, defined as the use of existing drugs for new therapeutic indications, has recently become an attractive strategy for new treatment approaches [3]. The Food and Drug Administration (FDA)-approved drug rafoxanide is a salicylanilide compound used in

veterinary medicine for the treatment of fascioliasis and some gastrointestinal roundworms in cattle and sheep [4–6]. Although the available evidence regarding the usage of the rafoxanide in humans is poor, a past study reported the therapeutic use of the drug in a seven-year-old girl affected by fascioliasis [7]. Recently, rafoxanide was identified as a potent inhibitor of the BRAF V600E mutant protein [8], which is important in CRC due to the fact that about 10% of CRCs harbor BRAF V600E mutations and the mutations are associated with a poorer prognosis for patients [9]. Mechanistically, the BRAF V600E mutated protein results in the constitutive activation of the mitogen-activated protein kinase (MAPK) pathway, leading to increased cell proliferation, survival and invasiveness [10,11]. In another study investigating the effects of anti-helminthic drugs on the hypervirulent stationary-phase of *Clostridium difficile* [12], rafoxanide showed no apparent toxicity on two human cell lines at concentrations up to 12.5 μ M and a markedly lower hemolytic activity compared to niclosamide [12], a FDA-approved drug for treatment of intestinal cestode in humans, and which has been

* Corresponding author. Department of Systems Medicine, University of “Tor Vergata” Via Montpellier, 1 00133, Rome, Italy.

E-mail address: carmine.stolfi@uniroma2.it (C. Stolfi).

¹ These authors contributed equally to the study.

reported to exert potent anti-cancer activities [13] and is currently undergoing a phase II clinical trial for metastatic CRC [14]. More recently, rafoxanide was shown to reduce proliferation and survival of human skin melanoma and squamous cell carcinoma cell lines by impairing the expression/activity of the cyclin-dependent kinases (CDK)4/6 [15], thus indicating the modulation of intracellular pathways other than RAF-MAPK could perhaps underlie in part the anti-cancer properties of the rafoxanide.

Altogether, such observations highlighted the possibility that rafoxanide might be repurposed as an anti-cancer agent for CRC patients, prompting us to investigate the potential anti-neoplastic properties of the drug on colon tumor cells *in vitro* and *in vivo*.

2. Materials and methods

2.1. Patients and samples

Paired tissue samples were taken from the tumor area and the macroscopically unaffected, adjacent, colonic mucosa of 5 patients who underwent colon resection for sporadic CRC (all with TNM stages II–III) at the Tor Vergata University Hospital (Rome, Italy). No patients received radiotherapy or chemotherapy before undergoing surgery. The human studies were approved by the local ethics committee and each patient gave written informed consent.

2.2. Animals

Apc^{min/+} mice, were obtained from Jackson (Bar Harbor, ME) and maintained in filter-topped cages on autoclaved food and water at the Plaisant animal facility (Rome, Italy). Mice were routinely tested (every 3 months) for health status and infections according to the Federation of European Laboratory Animal Science Associations (FELASA) guidelines. Mice resulted negative for all pathogens included in this protocol. Mice were also negative for *Helicobacter hepaticus* and *Helicobacter bilis*. All animal experiments were approved by the local Institutional Animal Care and Use Committee.

2.3. Cell culture

All reagents were from Sigma-Aldrich (Milan, Italy) unless specified. The human CRC cell lines HCT-116 and HT-29 were obtained from the American Type Culture Collection (ATCC, Manassas, VA) and maintained in McCoy's 5A medium supplemented with 10% fetal bovine serum (FBS) and 1% penicillin/streptomycin (P/S) (both from Lonza, Verviers, Belgium). The human CRC cell line DLD-1 was obtained from ATCC and maintained in RPMI 1640 medium supplemented with 10% FBS and 1% P/S. The human normal colonic epithelial cell line HCEC-1CT was obtained from EVERCYTE GmbH (Vienna, Austria) and maintained in ColoUp medium (EVERCYTE GmbH). NCM460, an epithelial cell line derived from the healthy colon mucosa of a 68-year-old Hispanic male [16], was obtained through a Material Transfer Agreement with INCELL (San Antonio, TX), and grown in M3:Base F medium (INCELL) supplemented with 10% FBS and 2.5 mM of D-glucose. Cell lines were recently authenticated by STR DNA fingerprinting using the PowerPlex 18D System kit according to the manufacturer's instructions (Promega, Milan, Italy). The STR profiles of all the cell lines matched the known DNA fingerprints. To determine whether the anti-proliferative effect of rafoxanide on CRC cells was reversible, HCT-116 and DLD-1 cells were treated with either rafoxanide or dimethyl sulfoxide (DMSO) (sham) for 24 h, then washed with PBS and cultured with fresh medium supplemented with either rafoxanide or DMSO for further 24 h. Cell proliferation was then assessed by 5-bromodeoxyuridine (BrdU) assay. To test whether the rafoxanide-mediated decrease of cyclin D1 was due to proteasome degradation, HCT-116 cells were pre-incubated or not with the proteasome inhibitor MG132 (Merck, Rome, Italy, used at 10 μM) for 1 h, and then stimulated with either DMSO (sham) or

2.5 μM rafoxanide for further 8 h. To assess the contribution of endoplasmic reticulum stress (ERS) in the anti-mitogenic effects of rafoxanide, CRC cells were pre-incubated for 1 h with either DMSO (sham) or the ERS alleviator tauroursodeoxycholic acid (TUDCA) (used at 200 μM) and stimulated or not with 2.5 μM rafoxanide for 0.5–24 h.

2.4. Assessment of cell proliferation, cycle distribution and death

Cell proliferation was assessed by using a commercially available BrdU assay kit (Roche Diagnostics, Monza, Italy). Briefly, 5000 cells were cultured in 96-well microplates and allowed to adhere overnight. Five-bromodeoxyuridine was added to the cell cultures 6 h before the end of the treatments and cell growth was evaluated by ELISA. For analysis of cell cycle distribution, cells were either left untreated or treated with rafoxanide or DMSO (sham). After 24 h, cells were pulsed with 10 mol/L BrdU for 60 min, fixed in 70% cold ethanol, and stored at 20 °C for at least 3 h. DNA was denatured in 2 mol/L HCl, and cells stained with anti-BrdU monoclonal antibody (Roche Diagnostics) followed by fluorescein isothiocyanate-conjugated secondary anti-mouse immunoglobulin G (Molecular Probes, Milan, Italy). After staining with 100 g/mL propidium iodide (PI), cells were analyzed by flow cytometry.

To score cell death, cells were either left untreated or treated with rafoxanide or DMSO (sham) for 24–60 h. Cells were then collected, washed twice in PBS, stained with FITC-annexin V (AV, 1:100 final dilution, Immunotools, Friesoyte, Germany) according to the manufacturer's instructions and incubated with 5 μg/ml PI for 30 min at 4 °C. Fluorescence was then measured using the FL-1 and FL-3 channels of Gallios (Beckman Coulter, Milan, Italy) flow cytometer. Viable cells were considered as AV-/PI- cells, apoptotic cells as AV+/PI- cells, while secondary necrotic cells were characterized by AV+/PI+ positive staining. In some experiments, HCT-116 and DLD-1 cells were pre-treated with the pan-caspase inhibitor Q-VD-OPH (R&D Systems, Minneapolis, MN, used at 10 μM) or DMSO (sham) for 1 h and then stimulated or not with 2.5 μM rafoxanide. Cell death was assessed by flow-cytometry after 48–60 h.

2.5. Measure of mitochondrial membrane potential

Mitochondrial membrane potential (MMP) variations were detected in HCT-116 and DLD-1 cells stimulated with either DMSO (sham) or 2.5 μM rafoxanide using the cyanine dye JC-1 (5,5',6,6'-tetrachloro-1,1',3,3'-tetraethylbenzimidazolocarbo-cyanine iodide) (Molecular Probes) according with the protocol described by Perelman et al. [17]. Valinomycin (Molecular Probes), an uncoupler of mitochondrial respiration, was used as positive control.

2.6. Western blotting

Protein extracts were prepared and run as described elsewhere [18]. Blots were incubated with antibodies against p-ERK (sc-7383), ERK1 (sc-271269), cyclin D1 (sc-20044), cyclin D2 (sc-53637), cyclin D3 (sc-182), cyclin-dependent kinase (CDK)4 (sc-601), CDK6 (sc-177), p-PERK (Thr-981) (sc-31577), PERK (sc-13073), eIF2α (sc-11386), GADD153/CHOP (sc-575) (1:500 final dilution; all from Santa Cruz Biotechnology, Inc., Dallas, TX), p-GCN2 (Thr-899) (ab75836, 1:500 final dilution, Abcam, Cambridge, UK), p-PKR (Thr446) (PA5-37704) and PKR (PA1-990) (1:1000 final dilution, both from Thermo Fisher Scientific), p-eIF2α (Ser51) (#3597), GCN2 (#3302) and cleaved Caspase-3 (Asp175) (#9664) (1:1000 final dilution, all from Cell signaling Technology, Danvers, MA) followed by a secondary antibody conjugated to horseradish peroxidase (1:20000, Dako, Santa Clara, CA). After analysis, each blot was stripped and incubated with a mouse-anti-human monoclonal β-actin antibody (1:5000 final dilution, A544) to ascertain equivalent loading of the lanes.

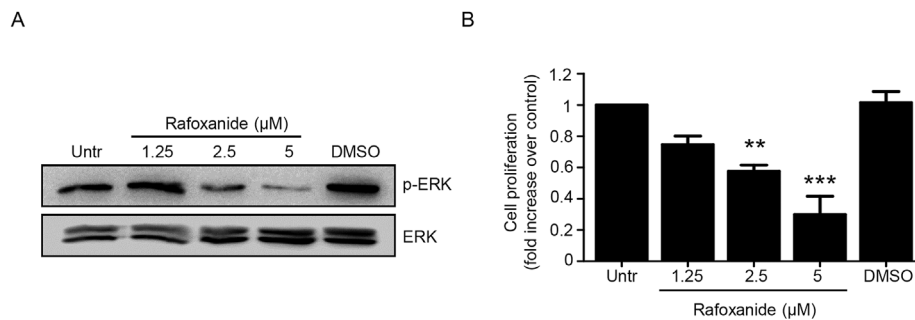


Fig. 1. Rafoxanide reduces *p*-ERK expression and inhibits proliferation in the CRC cell line HT-29, bearing the *BRAF V600E* mutation. (A) Cells were either left untreated or treated with rafoxanide or DMSO (sham) for 24 h. Protein extracts were evaluated for *p*-ERK and ERK expression by Western blotting. One of three representative experiments in which similar results were obtained is shown. (B) HT-29 cells were either left untreated (Untr) or treated with rafoxanide or DMSO (sham) for 24 h. Cell proliferation was assessed by 5-bromodeoxyuridine (BrdU) assay. Data indicate mean \pm SEM of three experiments. DMSO vs rafoxanide-treated cells: ***P* < 0.01, ****P* < 0.001.

2.7. RNA extraction, cDNA preparation and real-time PCR

Total RNA was extracted from cells and human CRC explants by using TRIzol reagent, according to the manufacturer's instructions (Life Technologies, Milan, Italy). A constant amount of RNA (1 μg /sample) was reverse-transcribed into complementary DNA (cDNA), and 1 μl of cDNA/sample was then amplified by real-time PCR using iQ SYBR Green Supermix (Bio-Rad Laboratories, Milan, Italy). Primers were as follows: cyclin D1: FWD: 5'-AGGCGGAGGAGAACAAACAG-3'; REV: 5'-CGGTAG TAGGACAGGAAGTTG-3', CHOP: FWD: 5'-GTCTAAGGCACT GAGCGTATC-3', REV: 5'-CCGAAGGAGAAAGGCAATGAC-3', GRP78: FWD: 5'-GGTGAAAGACCCTGACAAA-3', REV: 5'-GTCAGGCGATTCT GGTTCAT-3', spliced X-box binding protein 1 (XBP1s): FWD: 5'-TGCT GAGTCCGACGAGGTG-3', REV: 5'-GCTGGCAGGCTCTGGGAAG-3', β -actin: FWD: 5'-AAGATGACCCAGATCATGTTTGGAGACC-3', REV: 5'-AGCCAGTCCAGACGAGGAT-3'. Activating transcription factor 4 (ATF4) RNA expression was evaluated using a Taqman assay (Life Technologies). RNA expression was calculated relative to the house-keeping β -actin gene on the base of the $\Delta\Delta\text{Ct}$ algorithm.

2.8. Organ culture

For organ culture, CRC explants and adjacent non-tumor mucosa were placed on Millicell inserts (EMD Millipore, Milan, Italy) in a 6-well plate containing RPMI 1640 medium supplemented with 10% FBS, 1% P/S and 50 $\mu\text{g}/\text{ml}$ gentamycin in the presence of either DMSO (sham) or 5 μM rafoxanide for 24 h. The culture was performed in an organ culture chamber at 37 $^{\circ}\text{C}$ in a 5% $\text{CO}_2/95\%$ O_2 atmosphere.

2.9. Experimental model of sporadic CRC

Co-housed 6-7-wk-old female *Apc*^{min/+} mice received intraperitoneal injections of 10 mg/kg azoxymethane (AOM) once a week for 2 weeks in order to increase colon tumorigenesis as previously reported [19]. Two weeks after the last AOM injection mice were randomly divided in two groups and given either 7.5 mg/kg rafoxanide (in 10% DMSO in PBS) or 10% DMSO in PBS (sham) every other day by intraperitoneal injection until sacrifice (day 90). Body weight was recorded every week starting from day 21 until the end of the study. The dose of rafoxanide was selected in accordance with that currently used in veterinary treatment (i.e., 7.5–10 mg/kg). Colonoscopy was performed in a blinded manner for monitoring of tumorigenesis using the Coloview high-resolution mouse endoscopic system (Karl-Storz; Tuttlingen, Germany). Lesions observed during endoscopy were counted to obtain the overall number of lesions. Lesion sizes of all lesions in a given mouse were scored using the protocol described by Becker et al. [20].

2.10. Immunohistochemistry

Cryosections of human CRC explants and adjacent non-tumor mucosa were stained with a primary antibody directed against Ki-67 (clone

MIB-1, sc-101861, Santa Cruz Biotechnology, Inc.). Colonic cryosections of *Apc*^{min/+} mice were stained with H&E and neoplasms classified according with the guidelines described by Boivin and colleagues [21]. In parallel, sections were stained with Ki-67 (M7249, Dako), *p*-eIF2 α (Ser51) (#3597) and Cleaved Caspase-3 (Asp175) (both from Cell Signaling). Positive cells were visualized using MACH4 Universal HRP-Polymer kit with DAB (Biocare Medical, Pacheco, CA) and analyzed by LEICA DMI4000 B microscope using LEICA application suite software (V4.6.2).

2.11. Statistical analysis

Parametric data were analyzed using the two-tailed Student's t-test for comparison between two groups or one-way analysis of variance (ANOVA) followed by Tukey's post hoc test for multiple comparisons. Significance was defined as *P*-values < 0.05.

3. Results

3.1. Rafoxanide inhibits CRC cell growth

The epidermal growth factor receptor (EGFR)/RAS/RAF/mitogen-activated protein kinase kinase (MEK)/extracellular signal-regulated kinase (ERK) pathway plays a key role in the pathogenesis and progression of CRC [22]. As rafoxanide was recently described as a potent inhibitor of the oncogenic *BRAF V600E* mutant protein [8], we first tested the effect of this drug on EGFR/ERK pathway and proliferation in the CRC cell line HT-29, bearing the *BRAF V600E* mutation. Our data showed that rafoxanide inhibited ERK activation and *in vitro* growth in HT-29 cells in a dose-dependent fashion (Fig. 1A–B). Subsequently, we investigated whether rafoxanide could exert anti-proliferative effects also in human CRC cells bearing wild-type *BRAF* alleles (that is, HCT-116 and DLD-1). Of note, rafoxanide significantly reduced the growth of both cell lines (Fig. 2A). Such effects were fully reversible, because HCT-116 and DLD-1 cells proliferated regularly on removal of the compound (Suppl. Fig. 1). Importantly, rafoxanide did not significantly affect the proliferation of the human normal colon epithelial cell lines HCEC-1CT and NCM460 (Suppl. Fig. 2).

3.2. CRC cells accumulate in G0/G1 phase after rafoxanide exposure

We next assessed effects of rafoxanide on cell-cycle progression. The rafoxanide-induced CRC cell growth inhibition was associated with accumulation of cells in G0/G1 phase and decreased frequency of cells in S phase of the cell cycle (Fig. 2B). Cell cycle progression from G0/G1 to S phase is regulated by several D-type cyclins, together with the cyclin-dependent kinases 4 and 6 (CDK4 and CDK6) [23]. CRC cells stimulated with rafoxanide showed a striking decline in cyclin D1 protein levels (Fig. 2C). By contrast, there was no relevant change in the protein levels of cyclin D2 and cyclin D3 (Fig. 2C), thus indicating that loss of cyclin D1 in rafoxanide-treated cells was not due to generalized effects on cyclin D family members. A slight decrease in the levels of

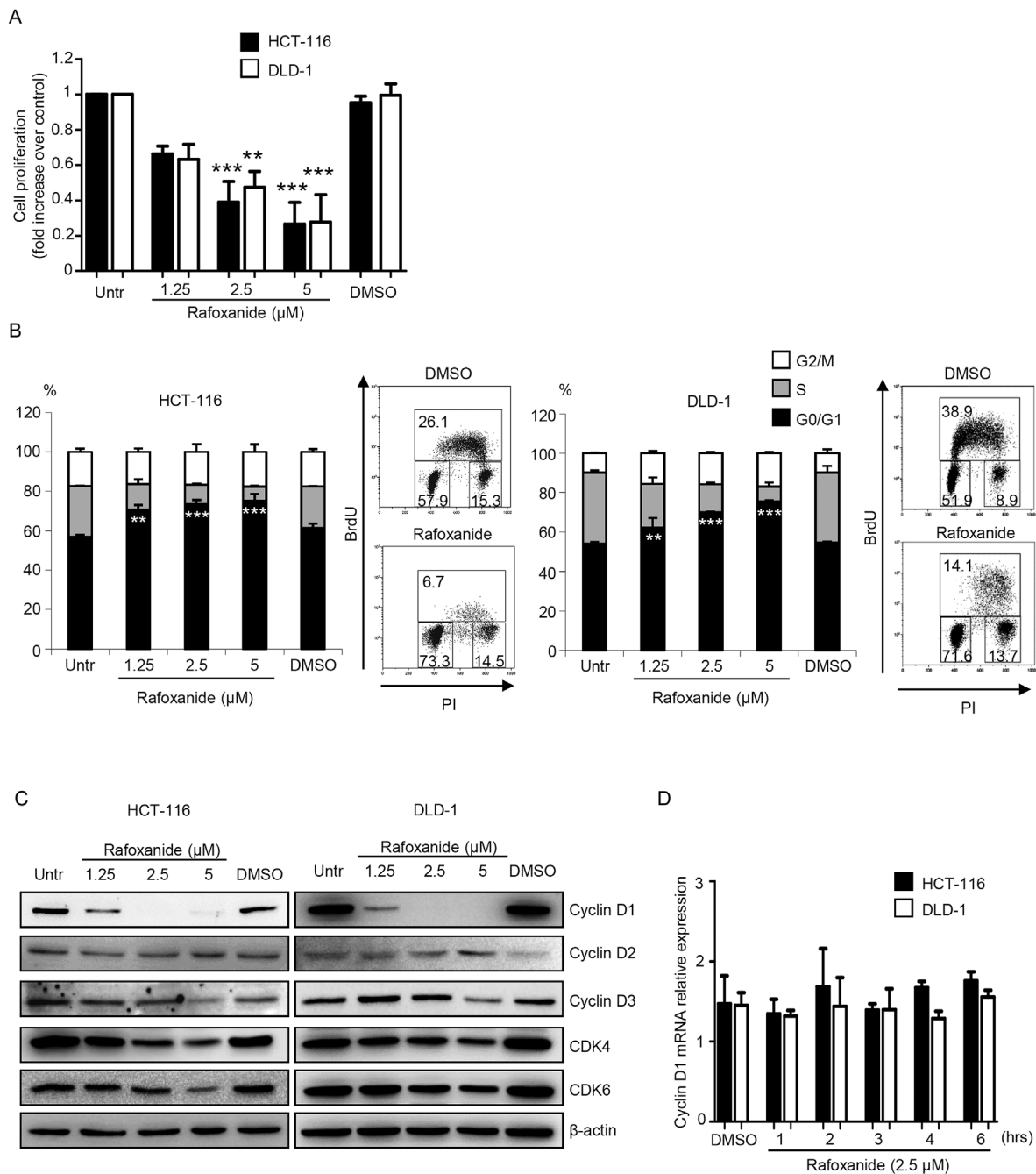
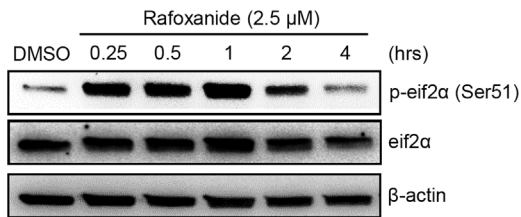


Fig. 2. The rafoxanide-mediated inhibition of CRC cell growth is associated with an accumulation of cells in G0/G1 phase of the cell cycle. (A) Rafoxanide inhibits the growth of the CRC cell lines HCT-116 and DLD-1, bearing wild-type *BRAF* alleles. Cells were either left untreated (Untr) or treated with either rafoxanide or DMSO (sham) for 24 h. Cell proliferation was assessed by 5-bromodeoxyuridine (BrdU) assay. Data indicate mean \pm SEM of four experiments (HCT-116: DMSO- vs rafoxanide-treated cells, ***P < 0.001; DLD-1: DMSO- vs rafoxanide-treated cells, **P < 0.01, ***P < 0.001). (B) Rafoxanide-treated cells accumulate in G0/G1 phase. HCT-116 and DLD-1 cells were treated or not with either rafoxanide or DMSO (sham) for 24 h. Values are the percentages of cells in the different phases of cell cycle and indicate mean \pm SEM of four experiments. A significant increase in the number of cells that accumulate in G0/G1 phase was seen in rafoxanide-treated cells compared with sham (**P < 0.01, ***P < 0.001). Right insets show representative dot-plots of the cell cycle distribution. (C) Rafoxanide down-regulates cyclin D1 protein levels. Total proteins from HCT-116 and DLD-1 cells treated as indicated in B were extracted and evaluated for cyclin D1, cyclin D2, cyclin D3, CDK4 and CDK6 expression by western blotting. β -actin was used as loading control. One of four representative experiments where similar results were obtained is shown. (D) Rafoxanide does not reduce cyclin D1 RNA expression. HCT-116 and DLD-1 cells were treated with either DMSO (sham) or rafoxanide for the indicated time points; cyclin D1 RNA transcripts were evaluated by real-time PCR. Levels are normalized to β -actin. Values are mean \pm SD of three experiments.

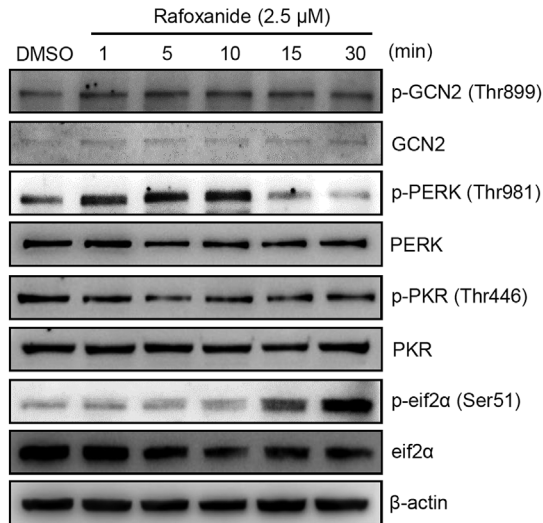
CDK4 and CDK6 was observed only at the higher doses of the drug (Fig. 2C). These findings are aligned with effects reported in the paper by Shi and colleagues, where rafoxanide was proposed as a dual CDK4/CDK6 inhibitor in melanoma and squamous cell carcinoma cell lines [15]. Treatment of HCEC-1CT cells with rafoxanide did not result in any relevant perturbation in cell cycle distribution or the levels of cyclin D1,

cyclin D2, cyclin D3, CDK4 or CDK6 protein expression (Suppl. Fig. 3A and B). No changes in cyclin D1 RNA transcripts were seen in either HCT-116 or DLD-1 cells after rafoxanide treatment, thus indicating that the inhibitory effects of rafoxanide on cyclin D1 expression were not at the transcriptional level (Fig. 2D). To test whether the rafoxanide-mediated decrease of cyclin D1 was due to proteasome degradation,

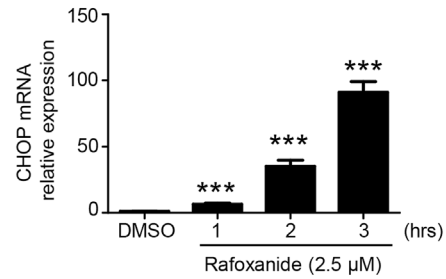
A



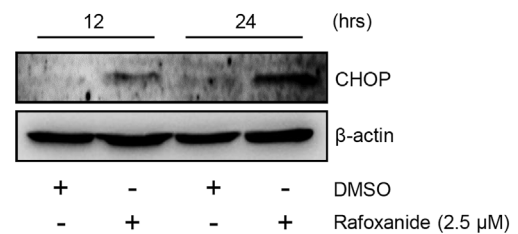
B



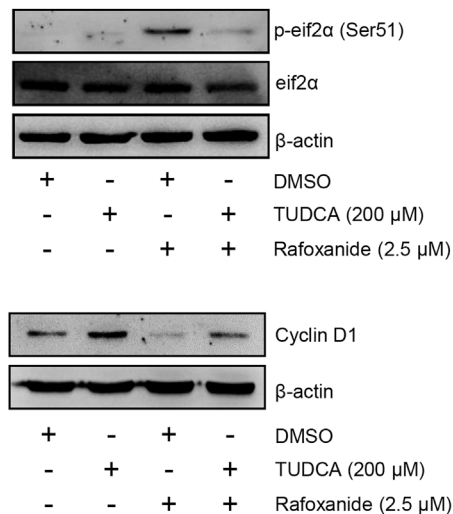
C



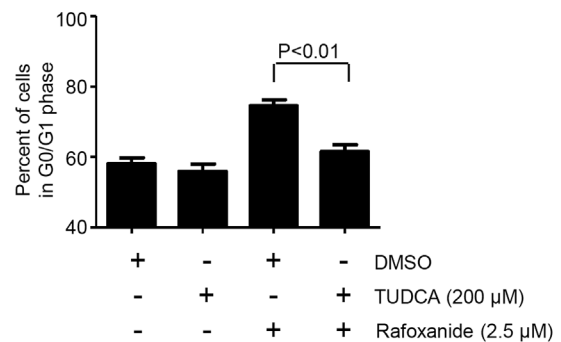
D



E



F



(caption on next page)

HCT-116 cells were pre-incubated with the proteasome inhibitor MG132 and then stimulated with either DMSO (sham) or rafoxanide. MG132 failed to rescue the rafoxanide-mediated Cyclin D1 down-regulation (Suppl. Fig. 4).

3.3. Rafoxanide promotes endoplasmic reticulum stress in CRC cells

Similar changes in cell proliferation, G0/G1 arrest and cyclin D1 protein expression have been described for cells exposed to agents that activate the endoplasmic reticulum stress (ERS) response, such as exposure of cells to hypoxia, low glucose levels, alterations of calcium homeostasis, accumulation of misfolded proteins, or other stresses [24].

Fig. 3. Rafoxanide promotes endoplasmic reticulum stress response in CRC cells. (A) Rafoxanide induces eIF2 α phosphorylation. Representative western blotting for p-eIF2 α (Ser51) and eIF2 α in extracts of HCT-116 cells treated with either DMSO (sham) or rafoxanide for the indicated time-points. One of three representative experiments in which similar results were obtained is shown. β -actin was used as loading control. (B) The rafoxanide-induced eIF2 α phosphorylation is preceded by PERK activation. Representative western blotting for p-GCN2 (Thr899), GCN2, p-PERK (Thr981), PERK, p-PKR (Thr446), PKR, p-eIF2 α (Ser51) and eIF2 α in extracts of HCT-116 cells treated with either DMSO (sham) or rafoxanide for the indicated time-points. One of three representative experiments in which similar results were obtained is shown. β -actin was used as loading control. (C) Rafoxanide enhances CHOP RNA expression. HCT-116 cells were treated with DMSO (sham) or rafoxanide for the indicated time points and CHOP transcripts evaluated by real-time PCR. Levels are normalized to β -actin. Values are mean \pm SD of three experiments (sham vs rafoxanide-treated cells, ***P < 0.001). (D) HCT-116 cells were treated with either DMSO (sham) or rafoxanide for the indicated time points. CHOP protein expression was evaluated by western blotting. One of three representative experiments in which similar results were obtained is shown. β -actin was used as loading control. (E) Tauroursodeoxycholic acid (TUDCA), an ERS alleviator, blocks eIF2 α phosphorylation and cyclin D1 down-regulation induced by rafoxanide. Total proteins extracted from HCT-116 cells cultured in the presence or absence of TUDCA for 1 h, and then treated with either DMSO (sham) or rafoxanide for 30 min or 24 h, were evaluated for p-eIF2 α and cyclin D1 respectively. One of three representative western blotting in which similar results were obtained is shown. (F) Treatment of HCT-116 cells with TUDCA reverses the rafoxanide-induced block of cell cycle in G0/G1 phase. Cells were cultured in the presence or absence of TUDCA for 1 h, and then treated with either DMSO (sham) or rafoxanide for further 24 h. The percentage of cells in G0/G1 phase was assessed by flow-cytometry. Values are mean \pm SEM of three experiments.

In particular, activation of PERK (PKR-like ER kinase) following ERS induction has been shown to phosphorylate/inactivate eIF2 α , an event that reduces the exchange of eIF2 α -GDP to eIF2 α -GTP required to deliver initiator met-tRNA_i^{Met} to the translation machinery and resulting in the specific inhibition of the synthesis of cell cycle regulators, such as cyclin D1 [25]. Thus, we assessed whether rafoxanide induced ERS. Treatment of CRC cells with rafoxanide promoted the phosphorylation of eIF2 α (Fig. 3A and Suppl. Fig. 5A), which was preceded by phosphorylation/activation of PERK but not that of other eIF2 α regulating kinases, namely GCN2 (general control non-derepressible-2) and PKR (protein kinase double-stranded RNA-dependent) (Fig. 3B), primarily activated in response to essential amino acid deprivation and viral infections respectively [26]. To further confirm that rafoxanide induced ERS in CRC cells, we assessed the expression of CCAAT/enhancer binding protein homologous transcription factor (CHOP), considered both an hallmark feature and a convenient readout of ERS [27]. Rafoxanide strongly induced CHOP RNA transcripts in both HCT-116 and DLD-1 cells (Fig. 3C). Notably, treatment of HCEC-1CT cells with rafoxanide barely increased eIF2 α phosphorylation and this event was associated with no change in CHOP mRNA expression (Suppl. Fig. 5A and B). Consistently with the up-regulation of CHOP RNA transcripts, rafoxanide treatment increased CHOP protein expression as compared to sham in both HCT-116 and DLD-1 cells (Fig. 3D and Suppl. Fig. 5C). Induction of ERS in rafoxanide-treated cells was also supported by enhanced RNA expression of other ERS biomarkers (i.e., XBP1s, ATF4 and GRP78) (Suppl. Fig. 6). Among the events that may lead to PERK activation and the resulting ERS cascade includes the perturbation of the mitochondrial homeostasis [28]. As rafoxanide was reported to be a potent uncoupling factor of mitochondrial oxidative phosphorylation [29], we evaluated whether rafoxanide induced ERS in CRC cells by affecting the mitochondrial membrane potential (MMP). However, time-course analysis clearly indicated that PERK activation was not preceded by a MMP decrease (Suppl. Fig. 7A and B). To link mechanistically the anti-mitogenic effect of rafoxanide with ERS induction, CRC cells were pre-incubated with TUDCA, a chemical chaperone reported to alleviate ERS in different cell compartments, including intestinal epithelial cells, via multiple mechanisms, such as by inhibiting the dissociation between GRP78 and PERK [30–32]. Notably, TUDCA potently inhibited rafoxanide-mediated eIF2 α phosphorylation as well as cyclin D1 protein downregulation and cell cycle arrest in G0/G1 phase (Fig. 3E–F). Altogether, our results indicate that rafoxanide negatively affects CRC cell growth through the induction of ERS, with resultant effects on cyclin D1 levels and cell cycle progression.

3.4. Rafoxanide induces CRC cell death

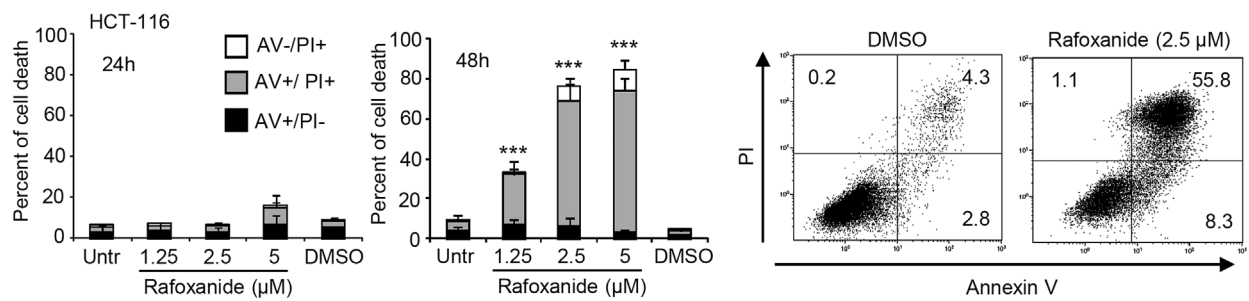
Because persistent cell cycle arrest in G0/G1 phase and unresolved ERS have been shown to be followed by activation of programmed cell death [33,34], we next evaluated whether prolonged treatment with rafoxanide influenced CRC cell survival. HCT-116 and DLD-1 cells were

treated with rafoxanide up to 48 and 60 h, respectively, and cell death was then assessed by flow cytometry. No significant change in the percentage of annexin V (AV)+ and/or propidium iodide (PI)+ cells was seen after 24-hr treatment with rafoxanide in either cell lines (Fig. 4A–B). However, analysis at later time points revealed that rafoxanide markedly increased the frequency of AV+ and/or PI+ cells (Fig. 4A–B). In contrast, rafoxanide treatment did not affect HCEC-1CT cell survival up to 60 h (Suppl. Fig. 8). Notably, pre-incubation of CRC cells with the pan-caspase inhibitor Q-VD-OPH totally reverted the rafoxanide-induced cell death (Fig. 4C), thus confirming the involvement of apoptotic pathway(s) in such processes.

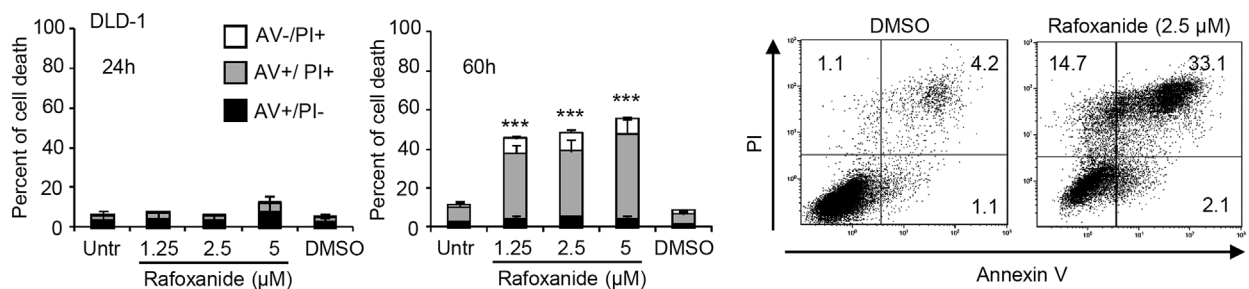
3.5. Rafoxanide reduces neoplastic cell proliferation in human CRC explants and colon carcinogenesis in *Apc*^{min/+} mice

To investigate whether rafoxanide was able to affect neoplastic cell growth *ex vivo*, human CRC explants were stimulated with the drug for 24 h and cell proliferation was evaluated by immunohistochemistry. Rafoxanide reduced the fraction of Ki-67-expressing CRC cells compared to sham (DMSO) treatment, while sparing non-transformed proliferating cells (Fig. 5A). The anti-mitogenic effect of rafoxanide observed in tumor explants was associated with ERS induction, as indicated by the increased expression of CHOP, GRP78 and ATF4 RNA expression compared to sham treatment (Fig. 5B). Next, we tested the ability of rafoxanide to inhibit intestinal tumor development *in vivo* using mice carrying a constitutional mutation in the *Adenomatous polyposis coli* (*Apc*) gene (*Apc*^{min/+} mice) and mimicking human sporadic CRC. Treatment of *Apc*^{min/+} mice with the carcinogen AOM increases tumor multiplicity and size as well as the frequency of invasive features of the tumor arising, particularly in the colon [19]. Mice were treated intraperitoneally with AOM (10 mg/kg) once a week for 2 weeks and monitored for tumor formation. Two weeks after the last AOM injection, mice received intraperitoneal injections of rafoxanide (7.5 mg/kg/mouse) or vehicle every other day, until euthanasia of the mice at the completion of the study (Fig. 6A). Endoscopy on day 88 showed that the sham-treated mice developed multiple large colonic lesions, whereas the number and size of lesions were reduced in the colon of rafoxanide-treated mice (Fig. 6B). No significant body weight changes were observed in mice treated with rafoxanide as compared with sham (Suppl. Fig. 9). At the time of euthanasia, lesions were detected in any of the sham-treated mice and distinguished as adenomas (28.6%), advanced adenomas (67.8%) or adenocarcinoma (3.6%). Conversely, only seven out of twelve mice treated with rafoxanide developed macroscopic lesions. These were classified as adenomas (60%) or advanced adenomas (40%). Immunohistochemistry for Ki-67 confirmed the anti-proliferative effect of rafoxanide on neoplastic cells (Fig. 6C). By contrast, there was no significant change in Ki-67 staining in the normal colonic mucosa of mice treated with the drug (Fig. 6C). Increased signal for p-eIF2 α , CHOP and cleaved caspase-3 was detected in tumor tissues of mice receiving rafoxanide compared to tumor tissues

A



B



C

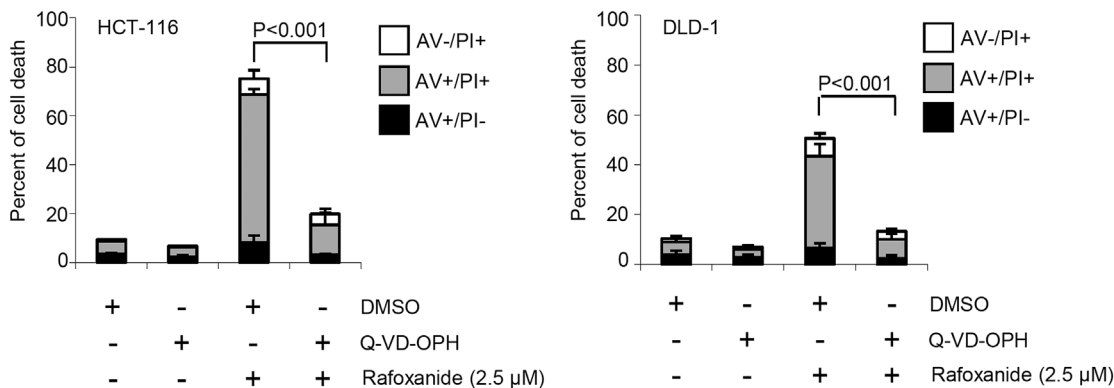


Fig. 4. Rafoxanide induces CRC cell death. (A) Representative histograms showing the percentage of cell death in HCT-116 cells either left untreated (Untr) or treated with either DMSO (sham) or rafoxanide for 24 h (left panel) and 48 h (right panel). Results indicate the percentage of cell death as assessed by flow-cytometry analysis of Annexin V (AV) and/or propidium iodide (PI)-positive cells. Data are expressed as mean ± SD of three experiments. Sham vs rafoxanide-treated cells, ***P < 0.001. Right inset. Representative dot-plots showing the percentages of AV- and/or PI-positive cells. (B) Representative histograms showing the percentage of cell death in DLD-1 cells either left untreated (Untr) or treated with either DMSO or rafoxanide for 24 h (left panel) and 60 h (right panel). Results indicate the percentage of cell death as assessed by flow-cytometry analysis of Annexin V (AV) and/or propidium iodide (PI)-positive cells. Data are expressed as mean ± SD of three experiments. Sham vs rafoxanide-treated cells, ***P < 0.001. Right inset. Representative dot-plots showing the percentages of AV- and/or PI-positive cells. (C) Q-VD-OPH, a pan-caspase inhibitor, blocks CRC cell death induced by rafoxanide. HCT-116 and DLD-1 cells were cultured in the presence or absence of Q-VD-OPH for 1 h, and then treated with either DMSO or rafoxanide for further 48 h (HCT-116) or 60 h (DLD-1). The percentages of AV- and/or PI-positive cells were assessed by flow cytometry. Data are mean ± SD of three experiments.

in sham-treated mice, whereas p-eIF2α, CHOP and cleaved caspase-3 expression was barely detectable in non-tumor colon epithelium of both the rafoxanide- and sham-treated groups (Fig. 7A–B and Suppl. Fig. 10). Collectively, these data confirm that rafoxanide induces ERS, inhibition of cell proliferation, and apoptosis in colon tumor tissues *in vivo*, but not in normal colonic epithelial cells.

4. Discussion

In this study we present data indicating that rafoxanide is a powerful inhibitor of CRC cell proliferation and survival. The anti-mitogenic action of rafoxanide was evident in CRC cells bearing both the *BRAF* V600E mutation as well as in CRC cells with wild-type *BRAF* alleles, but not in normal colonic epithelial cells. Thus, the findings provide

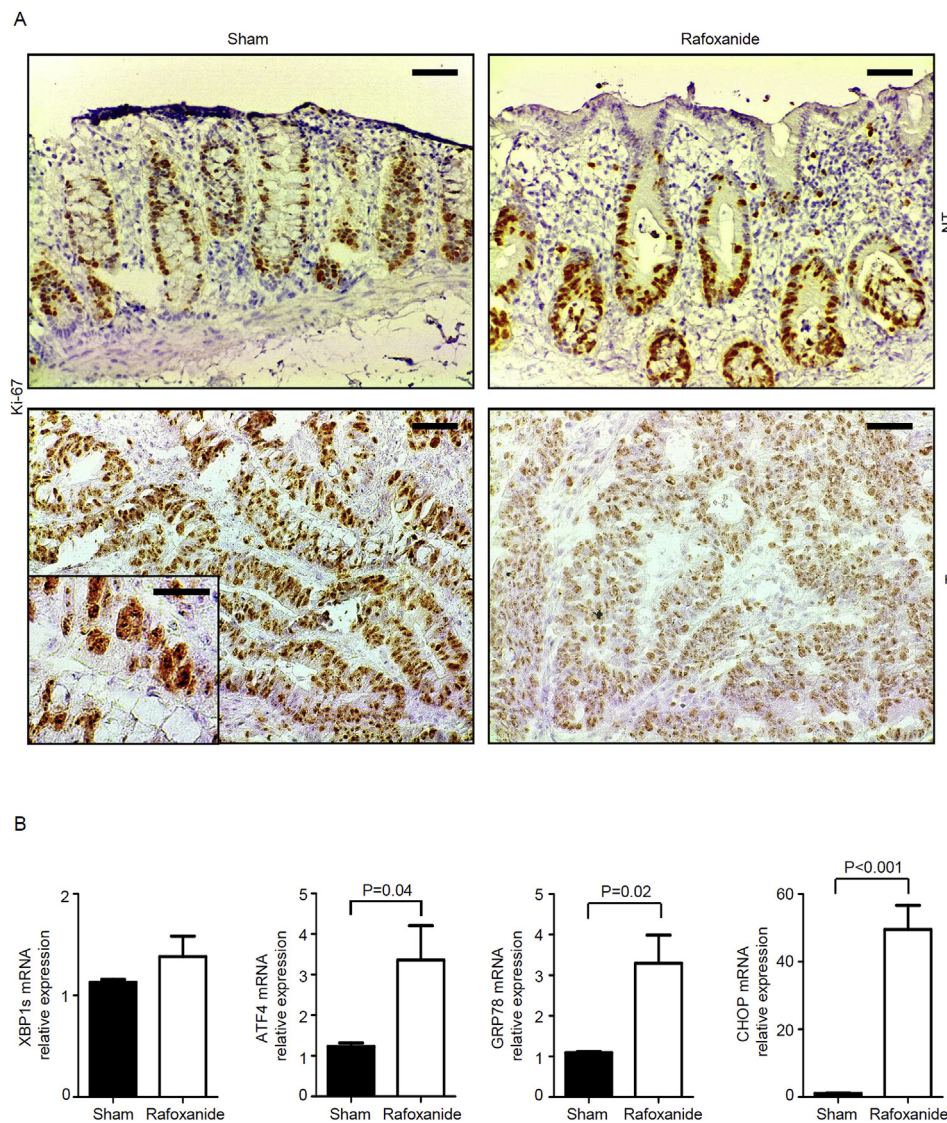


Fig. 5. Rafoxanide reduces the proliferation of neoplastic cells and induces ERS in human CRC explants. (A) Representative pictures of Ki-67-stained sections of freshly obtained CRC explant (T) and adjacent non-tumor mucosa (NT) treated with either DMSO (sham) or rafoxanide for 24 h. The scale bars are 20 μ m. The scale bars in the inset is 10 μ m. One of five representative experiments in which similar results were obtained is shown. (B) Representative histograms showing XBP1s, ATF4, GRP78 and CHOP RNA expression in human CRC explants treated as indicated in A. XBP1s, ATF4, GRP78 and CHOP RNA transcripts were evaluated by real-time PCR. Levels are normalized to β -actin. Values are mean \pm SD of three experiments.

evidence for preferential activity on CRC cells relative to normal cells, but not likely via effects on a BRAF mutation-dependent mechanism. The inhibitory effects of rafoxanide on CRC cells were associated with accumulation of cells in G0/G1 phase of the cell cycle and a marked decrease in cyclin D1 protein levels but not cyclin D1 RNA levels. Because marked reductions in cyclin D1 have previously been shown in response to induction of ERS, we next assessed whether rafoxanide triggered ERS in CRC cells. We found that rafoxanide activated the ERS cascade in CRC cells, as demonstrated by the phosphorylation/activation of PERK and eIF2 α as well as by the striking up-regulation of the downstream effector CHOP. In normal cells, which generally display no evidence of a significant ERS response, CHOP is barely expressed. Tumor cells often display negligible CHOP levels, despite a low/chronic ERS condition, because of the persistent activation/up-regulation of pro-survival components of the ERS response, such as the major ER chaperone protein GRP78/BiP [35]. Such ERS adaptive phenotype sets many tumor cells apart from normal cells and might therefore provide a tumor-specific target for potential therapeutic exploitation. Indeed, agents that are able to trigger further ERS may lead to the overload and subsequent breakdown of the ERS defense system in cancer cells thus resulting in cell cycle arrest and apoptosis [35], and a number of ERS inducing drugs are currently in clinical trials for cancer treatment [36–39]. Our data showed that rafoxanide strongly induced CHOP RNA transcripts in CRC but not in normal colonic epithelial cells. Thus, it is

tempting to speculate that the selectivity of the anti-neoplastic action of rafoxanide relies on the targeted aggravation of the pre-existing low/chronic ERS condition in CRC cells.

Among the stimuli and contexts that may induce ERS are perturbations of mitochondrial homeostasis [28]. As rafoxanide exerts its anti-helminthic effects by interfering with parasite mitochondrial ATP synthesis [29], to begin to uncover the mechanism/s underlying the rafoxanide-mediated ERS induction, we evaluated MMP in CRC cells following rafoxanide exposure. Our data clearly indicated that rafoxanide did not affect MMP at the same or earlier time points that those when PERK and eIF2 α phosphorylation were detected, thus ruling out a role of the mitochondria in such phenomenon. However, we cannot exclude the possibility that rafoxanide might affect the MMP of CRC cells at later time points and such an effect might have some contribution to rafoxanide-induced CRC cell death. Additional mechanisms by which a pharmacological agent can induce ERS are disturbances in calcium mobilization, perturbations of the proteasome machinery and protein folding/stability, modulation of reactive oxygen species signaling cascade, as well as inhibition of autophagy [40]. Future in-depth experimental work will be aimed at addressing whether the rafoxanide-mediated ERS induction relies on the modulation of one or more of the above-mentioned upstream events.

To determine the role of ERS in the anti-mitogenic effects of rafoxanide, CRC cells were stimulated with the drug in the presence of the

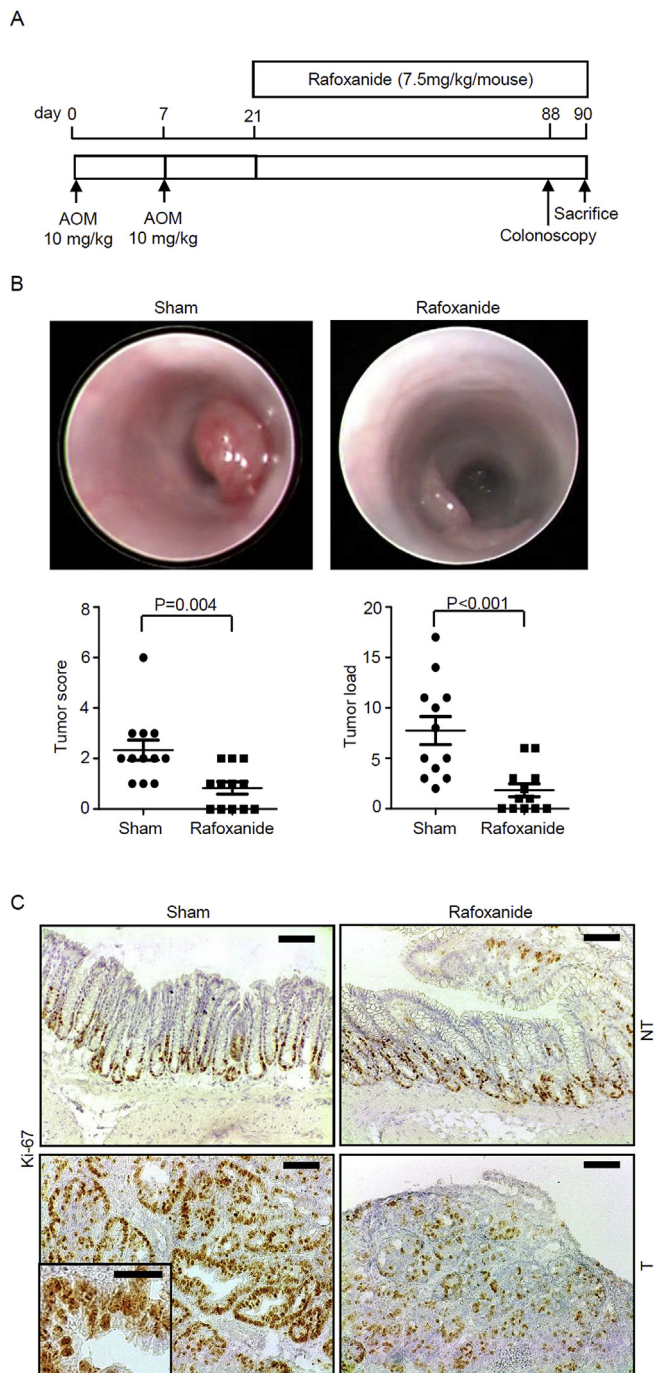


Fig. 6. Rafoxanide reduces colonic tumorigenesis in $Apc^{min/+}$ mice. (A) Experimental protocol used to assess the effect of rafoxanide treatment on colonic tumorigenesis in $Apc^{min/+}$ mice. (B) Upper panels show representative endoscopic pictures of colon lesions developed in mice treated with either DMSO (sham) or rafoxanide. Graphs show the number of lesions and the endoscopic scoring of lesions developed in mice treated with either DMSO (sham) or rafoxanide. Data indicate mean \pm SEM of three independent experiments in which at least four mice per group were considered. (C) Representative images showing Ki-67 immunostaining in colonic sections taken from $Apc^{min/+}$ mice treated with either DMSO (sham) or rafoxanide. The scale bars are 20 μ m. The scale bar in the inset is 10 μ m. One of five representative experiments in which similar results were obtained is shown. NT, non-tumor area, T, tumor area.

ERS alleviator TUDCA. Our results pinpointed the relevance of ERS induction in the rafoxanide-mediated cyclin D1 down-regulation and accumulation of cells in G0/G1 phase, in line with recent reports demonstrating an ability of TUDCA in mitigating the anti-neoplastic

effects of ERS-inducing agents/molecules in cancer cells [41–43]. Although CRC cells underwent death following rafoxanide treatment, this circumstance was seen only after 48- and 60-hr rafoxanide exposure in HCT-116 and DLD-1 cells respectively, thus indicating that induction of apoptosis followed the rafoxanide-induced cell growth arrest. We also showed that caspase activation was involved in the rafoxanide-induced CRC cell death, because pre-incubation of cells with a pan-caspase inhibitor conferred strong cytoprotection.

While this study was ongoing, Xiao and colleagues reported that rafoxanide inhibited proliferation and induced apoptosis in both wild type and *BRAF V600E* mutated multiple myeloma (MM) cells, while having no apparent cytotoxicity on normal peripheral blood mononuclear cells [44]. In line with our results, such an effect was associated with a cell cycle arrest in G0/G1 phase and a reduction of cyclin D1, CDK4 and CDK6 protein expression. In the same paper, the finding that rafoxanide caused synergistic cytotoxicity in MM cells in combination with bortezomib [44], a proteasome inhibitor recognized to promote ERS and approved for clinical use in MM patients [35], further supports our view that rafoxanide may exert its anti-neoplastic action by inducing ERS.

To extend our observations to primary human cells, we showed that rafoxanide reduced transformed epithelial cell proliferation in human CRC explants without substantially affecting the growth of normal colonic epithelial cells. We further strengthened our claims about the potential translational relevance of the anti-neoplastic effects of rafoxanide using an *in vivo* model of colon carcinogenesis. Systemic administration of rafoxanide reduced the multiplicity and size of lesions in $Apc^{min/+}$ mice. Consistent with our previous data, in the *in vivo* model, systemic administration of rafoxanide exerted anti-mitogenic effects and induced apoptosis in transformed but not in normal colonic epithelial cells. It is thus tempting to speculate that rafoxanide interferes preferentially with biological pathways that sustain malignant cell growth *in vivo*. In our mouse colon tumorigenesis model, rafoxanide would seem well-tolerated as no significant changes in body weight were observed in mice treated with the drug as compared with sham. Such observation is in line with the evidence reported by Xiao et al. in a MM xenograft model, showing no significant side effects of the drug in mice receiving intraperitoneal injections of 15 mg/kg rafoxanide every other day for 14 days [44]. However, further studies of dosage and long-term toxicity are needed to confirm the therapeutic potential and clinical benefit of rafoxanide. Further experimentation in murine models of CRC is ongoing to investigate whether rafoxanide, either alone or packaged in nanoparticles/liposomes, can inhibit colon carcinogenesis when orally administered.

In conclusion, we report the novel observations that rafoxanide is an ERS inducing agent with selective anti-tumor activity against CRC cells *in vitro* and *in vivo*. Importantly, to retain a tumor-selective cytotoxic outcome, the dose of rafoxanide should be chosen in order to sufficiently instigate ERS in tumor cells, but at the same time, only modestly trigger ERS in normal cells. Collectively, our data suggest that rafoxanide could potentially be deployed as an anti-cancer drug in CRC patients or as a chemoprevention agent in very selected patient populations at significantly elevated risk of developing clinically significant pre-cancerous and cancer lesions, perhaps such as in patients with familial adenomatous polyposis.

Author contributions

FL performed *in vitro* and *in vivo* experiments, analyzed data and contributed to write the manuscript, ADG analyzed data and performed most of the *in vitro* experiments; VDS, FC, AC, AO, EF, VD and DDF performed *in vitro* experiments; IM collected human samples and contributed to supervise parts of the project, ERF and GM critically revised the manuscript; CS was responsible for the study concept and design, performed the experiments, analyzed data, supervised the project and wrote the manuscript.

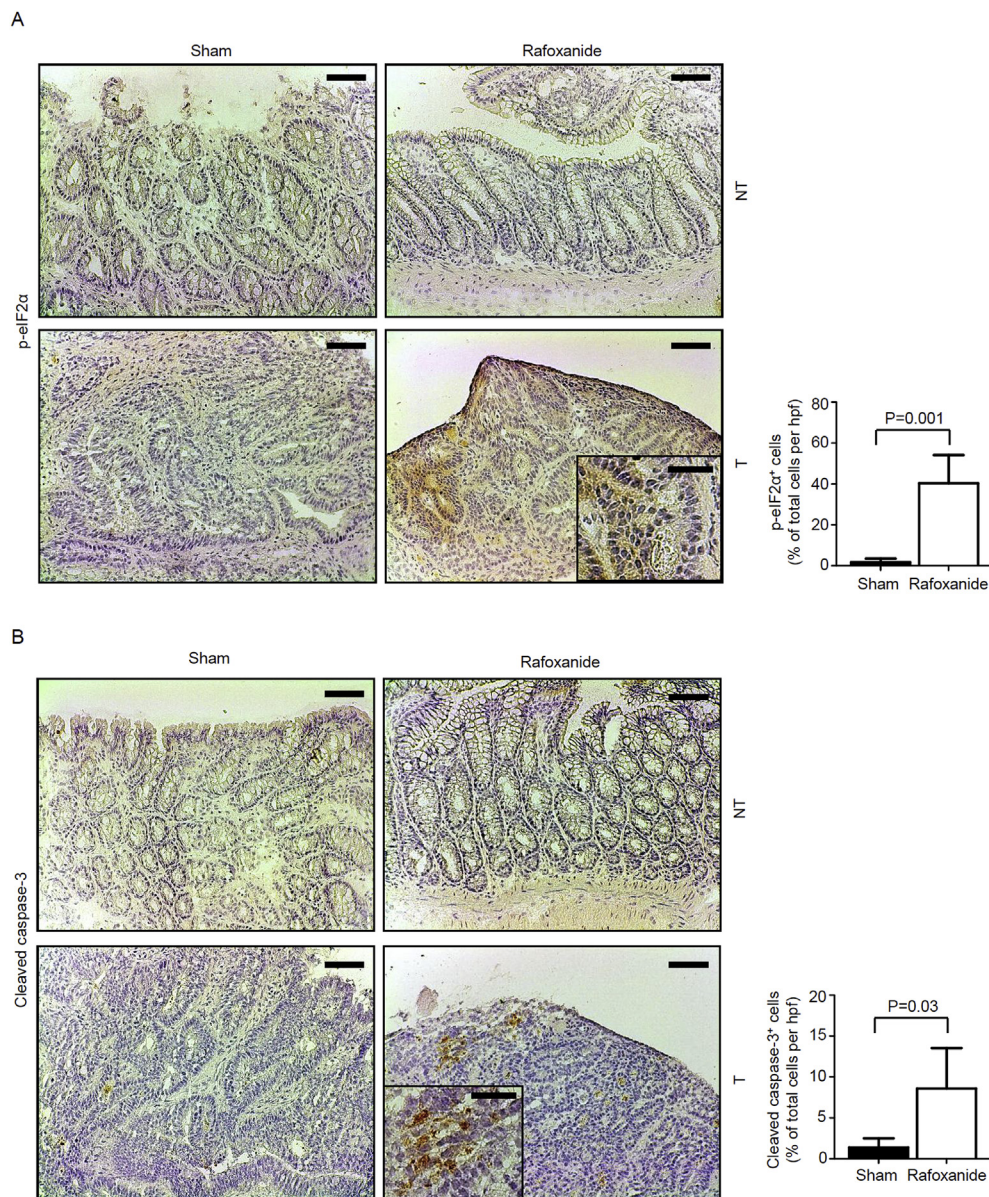


Fig. 7. Rafoxanide treatment induces eIF2 α phosphorylation and apoptosis in neoplastic colonic cells of *Apc*^{min/+} mice. (A–B) Representative images showing p-eIF2 α (Ser51)- (A) and cleaved caspase-3 positive cells (B) in colonic sections taken from *Apc*^{min/+} mice treated with either DMSO (sham) or rafoxanide and sacrificed at day 90. The scale bars are 20 μ m. The scale bar in the inset is 10 μ m. One of four representative experiments in which similar results were obtained is shown. Right insets. Quantification of p-eIF2 α (Ser51)- and cleaved caspase-3-positive epithelial cells in colonic sections taken from *Apc*^{min/+} mice treated with either DMSO (sham) or rafoxanide and sacrificed at day 90. Data are presented as mean values of positive cells per high power field (hpf) \pm SEM of two independent experiments in which at least two sections per group were analyzed. NT, non-tumor area, T, tumor area.

Conflicts of interest

GM has received consultant honoraria from AbbVie. The other authors declare no conflict of interest.

Acknowledgements

None.

Appendix A. Supplementary data

Supplementary data to this article can be found online at <https://doi.org/10.1016/j.canlet.2019.07.014>.

References

[1] H. Brenner, M. Kloor, C.P. Pox, Colorectal cancer, *Lancet* 383 (2014) 1490–1502.
 [2] W.A. Hammond, A. Swaika, K. Mody, Pharmacologic resistance in colorectal cancer: a review, *Ther. Adv. Med. Oncol.* 8 (2016) 57–84.
 [3] T.T. Ashburn, K.B. Thor, Drug repositioning: identifying and developing new uses for existing drugs, *Nature reviews, Drug discovery* 3 (2004) 673–683.
 [4] J. Armour, J. Corba, The anthelmintic activity of rafoxanide against immature

Fasciola hepatica in sheep, *Vet. Rec.* 87 (1970) 213–214.
 [5] S.E. Knapp, P.J. Presidente, Efficacy of rafoxanide against natural *Fasciola hepatica* infections in cattle, *Am. J. Vet. Res.* 32 (1971) 1289–1291.
 [6] G.E. Swan, The pharmacology of halogenated salicylanilides and their anthelmintic use in animals, *J. S. Afr. Vet. Assoc.* 70 (1999) 61–70.
 [7] M. Yurdakok, [Rafanoxide therapy in a child with fascioliasis], *Mikrobiyol. Bul.* 19 (1985) 38–40.
 [8] Y. Li, B. Guo, Z. Xu, B. Li, T. Cai, X. Zhang, Y. Yu, H. Wang, J. Shi, W. Zhu, Repositioning organohalogen drugs: a case study for identification of potent B-Raf V600E inhibitors via docking and bioassay, *Sci. Rep.* 6 (2016) 31074.
 [9] D. Barras, BRAF mutation in colorectal cancer: an update, *Biomarkers Canc.* 7 (2015) 9–12.
 [10] J.Y. Fang, B.C. Richardson, The MAPK signalling pathways and colorectal cancer, *the Lancet, Oncology* 6 (2005) 322–327.
 [11] J. Urošević, A.R. Nebreda, R.R. Gomis, MAPK signaling control of colon cancer metastasis, *Cell Cycle* 13 (2014) 2641–2642.
 [12] M. Gooyit, K.D. Janda, Reprofiled anthelmintics abate hypervirulent stationary-phase *Clostridium difficile*, *Sci. Rep.* 6 (2016) 33642.
 [13] Y. Li, P.K. Li, M.J. Roberts, R.C. Arend, R.S. Samant, D.J. Buchsbaum, Multi-targeted therapy of cancer by niclosamide: a new application for an old drug, *Cancer Lett.* 349 (2014) 8–14.
 [14] S. Burock, S. Daum, U. Keilholz, K. Neumann, W. Walther, U. Stein, Phase II trial to investigate the safety and efficacy of orally applied niclosamide in patients with metachronous or synchronous metastases of a colorectal cancer progressing after therapy: the NIKOLO trial, *BMC Canc.* 18 (2018) 297.
 [15] X. Shi, H. Li, A. Shi, H. Yao, K. Ke, C. Dong, Y. Zhu, Y. Qin, Y. Ding, Y.H. He, X. Liu, L. Li, L. Lei, Q. Hai, W. Chen, K.S. Leung, M.H. Wong, H.F. Kung, M.C. Lin,

- Discovery of rafoxanide as a dual CDK4/6 inhibitor for the treatment of skin cancer, *Oncol. Rep.* 40 (2018) 1592–1600.
- [16] M.P. Moyer, L.A. Manzano, R.L. Merriman, J.S. Stauffer, L.R. Tanzer, NCM460, a normal human colon mucosal epithelial cell line, in vitro cellular & developmental biology, *Animal* 32 (1996) 315–317.
- [17] A. Perelman, C. Wachtel, M. Cohen, S. Haupt, H. Shapiro, A. Tzur, JC-1: alternative excitation wavelengths facilitate mitochondrial membrane potential cytometry, *Cell Death Dis.* 3 (2012) e430.
- [18] C. Stolfi, D. Fina, R. Caruso, F. Caprioli, M. Sarra, M.C. Fantini, A. Rizzo, F. Pallone, G. Monteleone, Cyclooxygenase-2-dependent and -independent inhibition of proliferation of colon cancer cells by 5-aminosalicylic acid, *Biochem. Pharmacol.* 75 (2008) 668–676.
- [19] V. De Simone, E. Franze, G. Ronchetti, A. Colantoni, M.C. Fantini, D. Di Fusco, G.S. Sica, P. Sileri, T.T. Macdonald, F. Pallone, G. Monteleone, C. Stolfi, Th17-type cytokines, IL-6 and TNF- α synergistically activate STAT3 and NF- κ B to promote colorectal cancer cell growth, *Oncogene* 34 (2015) 3493–3503.
- [20] C. Becker, M.C. Fantini, S. Wirtz, A. Nikolaev, R. Kiesslich, H.A. Lehr, P.R. Galle, M.F. Neurath, In vivo imaging of colitis and colon cancer development in mice using high resolution chromoendoscopy, *Gut* 54 (2005) 950–954.
- [21] G.P. Boivin, K. Washington, K. Yang, J.M. Ward, T.P. Pretlow, R. Russell, D.G. Besselsen, V.L. Godfrey, T. Doetschman, W.F. Dove, H.C. Pitot, R.B. Halberg, S.H. Itzkowitz, J. Groden, R.J. Coffey, Pathology of mouse models of intestinal cancer: consensus report and recommendations, *Gastroenterology* 124 (2003) 762–777.
- [22] P.J. Roberts, C.J. Der, Targeting the Raf-MEK-ERK mitogen-activated protein kinase cascade for the treatment of cancer, *Oncogene* 26 (2007) 3291–3310.
- [23] G.I. Shapiro, Cyclin-dependent kinase pathways as targets for cancer treatment, *J. Clin. Oncol. : Off. J. Am. Soc. Clin. Oncol.* 24 (2006) 1770–1783.
- [24] J. Wu, R.J. Kaufman, From acute ER stress to physiological roles of the Unfolded Protein Response, *Cell Death Differ.* 13 (2006) 374–384.
- [25] J.W. Brewer, L.M. Hendershot, C.J. Sherr, J.A. Diehl, Mammalian unfolded protein response inhibits cyclin D1 translation and cell-cycle progression, *Proc. Natl. Acad. Sci. U. S. A* 96 (1999) 8505–8510.
- [26] N. Donnelly, A.M. Gorman, S. Gupta, A. Samali, The eIF2 α kinases: their structures and functions, *Cell. Mol. Life Sci. : CM* 70 (2013) 3493–3511.
- [27] S. Oyadomari, M. Mori, Roles of CHOP/GADD153 in endoplasmic reticulum stress, *Cell Death Differ.* 11 (2004) 381–389.
- [28] A.R. van Vliet, P. Agostinis, Mitochondria-associated membranes and ER stress, *Curr. Top. Microbiol. Immunol.* 414 (2018) 73–102.
- [29] R.J. Martin, Modes of action of anthelmintic drugs, *Vet. J.* 154 (1997) 11–34.
- [30] E. Berger, D. Haller, Structure-function analysis of the tertiary bile acid TUDCA for the resolution of endoplasmic reticulum stress in intestinal epithelial cells, *Biochem. Biophys. Res. Commun.* 409 (2011) 610–615.
- [31] S. Vang, K. Longley, C.J. Steer, W.C. Low, The unexpected uses of urso- and tauroursodeoxycholic acid in the treatment of non-liver diseases, *Global. Adv. Health. Med.* 3 (2014) 58–69.
- [32] Y.M. Yoon, J.H. Lee, S.P. Yun, Y.S. Han, C.W. Yun, H.J. Lee, H. Noh, S.J. Lee, H.J. Han, S.H. Lee, Tauroursodeoxycholic acid reduces ER stress by regulating of Akt-dependent cellular prion protein, *Sci. Rep.* 6 (2016) 39838.
- [33] R. Sano, J.C. Reed, ER stress-induced cell death mechanisms, *Biochim. Biophys. Acta* 1833 (2013) 3460–3470.
- [34] C. Stolfi, M. Sarra, R. Caruso, M.C. Fantini, D. Fina, R. Pellegrini, G. Palmieri, T.T. Macdonald, F. Pallone, G. Monteleone, Inhibition of colon carcinogenesis by 2-methoxy-5-amino-N-hydroxybenzamide, a novel derivative of mesalamine, *Gastroenterology* 138 (2010) 221–230.
- [35] A.H. Schonthal, Endoplasmic reticulum stress and autophagy as targets for cancer therapy, *Cancer Lett.* 275 (2009) 163–169.
- [36] A. Drilon, A.J. Schoenfeld, K.C. Arbour, A. Litvak, A. Ni, J. Montecalvo, H.A. Yu, E. Panora, L. Ahn, M. Kennedy, A. Haughney-Siller, V. Miller, M. Ginsberg, M. Ladanyi, M. Arcila, N. Rekhtman, M.G. Kris, G.J. Riely, Exceptional responders with invasive mucinous adenocarcinomas: a phase 2 trial of bortezomib in patients with KRAS G12D-mutant lung cancers, *Cold Spring Harb. Mol. Case Stud.* 5 (2019).
- [37] E.E. Manasanch, J.J. Shah, H.C. Lee, D.M. Weber, S.K. Thomas, B. Amini, L. Feng, Z. Berkova, M. Hildebrandt, R.Z. Orłowski, Bortezomib, lenalidomide, and dexamethasone with panobinostat for front-line treatment of patients with multiple myeloma who are eligible for transplantation: a phase 1 trial, *the Lancet, Haematology* 5 (2018) e628–e640.
- [38] M.R. Becnel, L.J. Nastoupil, F. Samaniego, R.E. Davis, M.J. You, M. Green, F.B. Hagemeister, M.A. Fanale, L.E. Fayad, J.R. Westin, M. Wang, Y. Oki, S.G. Forbes, L. Feng, S.S. Neelapu, N.H. Fowler, Lenalidomide plus rituximab (R2) in previously untreated marginal zone lymphoma: subgroup analysis and long-term follow-up of an open-label phase 2 trial, *Br. J. Haematol.* 185 (5) (2019) 874–882, <https://doi.org/10.1111/bjh.15843>.
- [39] A. Davies, T.E. Cummin, S. Barrans, T. Maishman, C. Mamot, U. Novak, J. Caddy, L. Stanton, S. Kazmi-Stokes, A. McMillan, P. Fields, C. Pocock, G.P. Collins, R. Stephens, F. Cucco, A. Clipson, C. Sha, R. Tooz, M.A. Care, G. Griffiths, M.Q. Du, D.R. Westhead, C. Burton, P.W.M. Johnson, Gene-expression profiling of bortezomib added to standard chemoimmunotherapy for diffuse large B-cell lymphoma (REMoDL-B): an open-label, randomised, phase 3 trial, *Lancet Oncol.* 20 (5) (2019) 649–662, [https://doi.org/10.1016/S1470-2045\(18\)30935-5](https://doi.org/10.1016/S1470-2045(18)30935-5).
- [40] S.J. Healy, A.M. Gorman, P. Mousavi-Shafaei, S. Gupta, A. Samali, Targeting the endoplasmic reticulum-stress response as an anticancer strategy, *Eur. J. Pharmacol.* 625 (2009) 234–246.
- [41] B. Tan, R. Jia, G. Wang, J. Yang, Astragaloside attenuates the progression of prostate cancer cells through endoplasmic reticulum stress pathways, *Oncology letters* 16 (2018) 3901–3906.
- [42] T. Arbel Rubinstein, S. Shahmoon, E. Zigmund, T. Etan, K. Merenbakh-Lamin, M. Pasmanik-Chor, G. Har-Zahav, I. Barshack, G.W. Vainer, N. Skalka, R. Rosin-Arbesfeld, C. Varol, T. Rubinek, I. Wolf, Klothe suppresses colorectal cancer through modulation of the unfolded protein response, *Oncogene* 38 (2019) 794–807.
- [43] Q. Feng, H. Wang, J. Pang, L. Ji, J. Han, Y. Wang, X. Qi, Z. Liu, L. Lu, Prevention of wogonin on colorectal cancer tumorigenesis by regulating p53 nuclear translocation, *Front. Pharmacol.* 9 (2018) 1356.
- [44] W. Xiao, Z. Xu, S. Chang, B. Li, D. Yu, H. Wu, Y. Xie, Y. Wang, B. Xie, X. Sun, Y. Kong, X. Lan, W. Bu, G. Chen, L. Gao, X. Wu, J. Shi, W. Zhu, Rafoxanide, an organohalogen drug, triggers apoptosis and cell cycle arrest in multiple myeloma by enhancing DNA damage responses and suppressing the p38 MAPK pathway, *Cancer Lett.* 444 (2019) 45–59.